Geochemistry, Geophysics, Geosystems®

AGU ADVANCING EARTH AND SPACE SCIENCES

RESEARCH ARTICLE
10.1029/2024GC011795

Rhenium Isotopes Record Oxidative Weathering Intensity in Sedimentary Rocks

A. J. Dickson[1], R. G. Hilton[2], J. Prytulak[3], D. Minisini[4,5], J. S. Eldrett[6], M. Dellinger[7], M. Stow[2], and W. Wang[1,8]

[1]Centre of Climate, Ocean and Atmosphere, Department of Earth Sciences, Royal Holloway University of London, Egham, UK, [2]Department of Earth Sciences, University of Oxford, Oxford, UK, [3]Department of Earth Sciences, Durham University, Durham, UK, [4]Department of Earth, Environmental, and Planetary Sciences, Rice University, Houston, TX, USA, [5]ExxonMobil, Spring, TX, USA, [6]School of Ocean and Earth Sciences, National Oceanography Centre, University of Southampton, Southampton, UK, [7]Environnements Dynamiques et Territoires de la Montagne (EDYTEM), CNRS—Université Savoie Mont-Blanc, Le Bourget du Lac, France, [8]Now at School of Marine Sciences, Sun Yat-sen University, Zhuhai, China

Abstract Oxidative weathering of organic carbon in sedimentary rocks is a major source of CO_2 to the atmosphere over geological timescales, but the size of this emission pathway in Earth's past has not been directly quantified due to a lack of available proxy approaches. We have measured the rhenium isotope composition of organic-rich rocks sampled from unweathered drill cores and weathered outcrops in south Texas, whose stratigraphic successions can be tightly correlated. Oxidative weathering of more than 90% of the organic carbon and ∼85% of the rhenium is accompanied by a shift to lower rhenium isotope compositions in the weathered outcrops. The calculated isotope composition of rhenium weathered from the initial bedrock for individual samples varies systematically by ∼0.7‰ with different fractions of rhenium loss. This variation can be empirically modeled with isotope fractionation factors of $\alpha = 1.0002–1.0008$. Our results indicate that the isotope composition of rhenium delivered to the oceans can be altered by weathering intensity of rock organic matter and that the rhenium isotope composition of seawater is sensitive to past oxidative weathering and associated CO_2 emissions.

Plain Language Summary Carbon dioxide is emitted into the atmosphere when sedimentary rocks containing ancient organic carbon are exposed to oxygen. This process, referred to as oxidative weathering, is an important part of the global carbon cycle that may play a vital role in climate change over geological timescales. In this study, we have investigated whether it is possible to use the isotope composition of rhenium metal as a proxy for this oxidation process since rhenium is liberated from rocks alongside organic carbon. Our findings show that the rhenium removed from rocks during weathering has an isotopic fingerprint that is linked to the degree of weathering—and thus presumably to the extent of carbon oxidation. There are several important features of rhenium isotope behavior that are still underconstrained, not least where Re resides in organic rich rocks, but our findings nonetheless advance an emerging approach to reconstructing the ancient carbon cycle.

Key Points:

- Oxidative weathering removes isotopically heavy rhenium from organic-rich sedimentary rocks
- The isotopic composition of weathered rhenium changes with weathering intensity
- Rhenium isotopes may trace variations in oxidative weathering intensity, and hence, oxidative CO_2 emission fluxes in the Earth's ancient past

Supporting Information:

Supporting Information may be found in the online version of this article.

Correspondence to:

A. J. Dickson,
alex.dickson@rhul.ac.uk

Citation:

Dickson, A. J., Hilton, R. G., Prytulak, J., Minisini, D., Eldrett, J. S., Dellinger, M., et al. (2024). Rhenium isotopes record oxidative weathering intensity in sedimentary rocks. *Geochemistry, Geophysics, Geosystems*, *25*, e2024GC011795. https://doi.org/10.1029/2024GC011795

Received 31 JUL 2024
Accepted 4 OCT 2024

Author Contributions:

Conceptualization: A. J. Dickson, R. G. Hilton, J. Prytulak
Formal analysis: A. J. Dickson, D. Minisini
Funding acquisition: A. J. Dickson, R. G. Hilton, J. Prytulak
Investigation: A. J. Dickson, D. Minisini
Methodology: A. J. Dickson, R. G. Hilton
Project administration: A. J. Dickson, R. G. Hilton
Resources: A. J. Dickson, R. G. Hilton, D. Minisini, J. S. Eldrett
Validation: A. J. Dickson, R. G. Hilton, J. Prytulak, D. Minisini, J. S. Eldrett, M. Dellinger, M. Stow, W. Wang

1. Introduction

Earth's long-term climate state is regulated by the weathering of crustal rocks. Silicate weathering has the capacity to remove atmospheric CO_2 over timescales of $10^{3–6}$ years and is recognized as the primary negative feedback on mantle CO_2 emissions in long-term climate simulations (Archer, 2005; Lenton et al., 2018; Walker et al., 1981). However, oxidative weathering of organic carbon (OC) in sedimentary rocks—variously referred to as either kerogen or petrogenic carbon—has been shown to account for CO_2 emissions to the atmosphere that are similar or greater in magnitude to global silicate weathering fluxes (Hilton & West, 2020; Zondervan et al., 2023). Modern day estimates of CO_2 fluxes from oxidative weathering have been calculated by taking advantage of the close empirical association between rhenium (Re) and OC concentrations in sedimentary rocks (Dalai et al., 2002) by measuring the flux of Re transported through rivers and equating this to OC loss using a Re:OC stoichiometry obtained from measurements of catchment rocks and/or riverine bedloads (Hilton et al., 2014). This approach has been critical in determining the size of modern oxidative CO_2 emissions (Dellinger et al., 2023; Hilton et al., 2021) and their comparison to silicate weathering fluxes (Horan et al., 2019; Zondervan et al., 2023). This approach cannot, however, be used to quantify emissions in the geological past due to our inability to sample

Writing – original draft: A. J. Dickson
Writing – review & editing: R. G. Hilton, J. Prytulak, D. Minisini, J. S. Eldrett, M. Dellinger, M. Stow, W. Wang

rivers from millions of years ago. The lack of proxy approaches to quantify past oxidative CO_2 emissions means that the contribution of this flux to global paleoclimate changes is not well known. Recent studies have, however, attempted to quantify emissions for transient climate events such as the Paleocene Eocene Thermal Maximum using biomarkers for recalcitrant organic matter reworked into marine sediments (Hollingsworth et al., 2024; Lyons et al., 2017).

An alternative approach is to use the Re isotope system to reconstruct the weathering intensity of rock OC (expressed as δ^{187}Re relative to NIST SRM 3143: $((^{187}Re/^{185}Re_{sample}/^{187}Re/^{185}Re_{NIST3143}) - 1)*1{,}000$). Hints from a black shale weathering profile (Miller et al., 2015) and the isotope composition of river waters and sediments in regions draining sedimentary rocks (Dellinger et al., 2021) suggest that the Re isotope system may be sensitive to weathering intensity. In this contribution, we explore the relationship between the Re isotope system and oxidative weathering by determining (a) whether oxidative weathering produces a measurable shift in the δ^{187}Re composition of sedimentary rocks, (b) whether the δ^{187}Re of Re liberated by oxidative weathering can vary as a function of weathering intensity (which we define here as the fraction of Re loss) and (c) whether the magnitude of Re isotope fractionation during weathering has the potential to alter the well-mixed global seawater Re isotope composition over geological timescales. The sample set we employ for this purpose has been obtained from the Late Cretaceous age Eagle Ford Group of South Texas (Figure 1). This succession of organic-rich mudrocks has a highly detailed regional lithostratigraphic framework that allows the correlation of outcrop samples exposed to variable levels of surface oxidation with unweathered drillcore samples at a bed-to-bed scale of generally better than 1–2 m (Figure 2, Table 1, Minisini et al., 2018). This framework allows a direct calculation of the isotopic composition of Re mobilized by oxidative weathering using a mass-balance approach. Unweathered samples come from the Innes-1 drillcore and weathered samples come from two outcrops (DR5 and DR12) (Figures 1 and 2).

2. Materials and Methods

Dry rock samples were initially powdered in an agate mill. For concentration measurements, 50 mg powder aliquots were mixed with a ^{185}Re spike solution and dissolved completely in 3:1 concentrated HNO_3 and HCl acid, then in 2:1 HNO_3 and HF acid. The residues were redissolved in 2M HNO_3 and Re was separated for mass spectrometry using amyl-alcohol extraction (Birck et al., 1997). Rhenium ratios were measured using a Neptune Plus MC-ICP-MS and corrected for instrumental mass fractionation by addition of 30 ng g^{-1} W (NIST SRM 3163). Concentrations were calculated by isotope dilution using the $^{185}Re/^{187}Re$ ratios. Samples for δ^{187}Re analysis were initially ashed in clean porcelain crucibles at 450°C to remove organic matter.

Sufficient powder mass to obtain several ng Re was then weighed into acid-clean Teflon vials and digested in 2:1 HNO_3 and HF acid, then 6M HCl for several days to dissolve fluorides. Finally, the sample digests were evaporated to dryness and redissolved in 1M HCl. Rhenium was separated from matrix elements using a 3-stage chromatography procedure modified from Dickson et al. (2020) and Dellinger et al. (2020). Stage one columns utilized 2 ml AG1-X8 anion resin (200–400 mesh). Samples were loaded in 1M HCl (10 ml acid per 0.5 g dissolved rock) followed by 2 × 10 ml rinses of 1M HCl to elute matrix elements. 3 ml of 3M HNO_3 was subsequently used to elute transition metals, before 14 ml 7.5M HNO_3 to elute Re into clean Teflon. Stage two and three columns were utilized 200 µl AG1-X8 resin loaded onto Teflon columns. Samples were loaded in 1 ml 1M HCl, followed by 2 × 1 ml additions of 1M HCl and 0.3 ml 3M HNO_3. Rhenium was finally eluted in 5 ml 3M HNO_3.

Purified samples were diluted to between 2 and 4 ppb, doped with 30 ppb W to correct for instrumental mass fractionation and measured using a Neptune Plus MC-ICP-MS equipped with 10^{13} Ω resistors using the same method of Dickson et al. (2020). Each measurement consisted of 40 × 8.4 s cycles and consumed ~1.3–2.6 ng Re. NIST SRM 989 was measured throughout the analytical sessions used for this study (June 2021–February 2024) and had a long-term average of −0.26 ± 0.1‰ (2 S.D., $n = 69$), which is within the uncertainty of the values presented by Miller et al. (2009), Dickson et al. (2020), and Dellinger et al. (2020). Rhenium procedural blanks were consistently <20 pg and sample recovery through the column procedure was always >65%, and typically >80%.

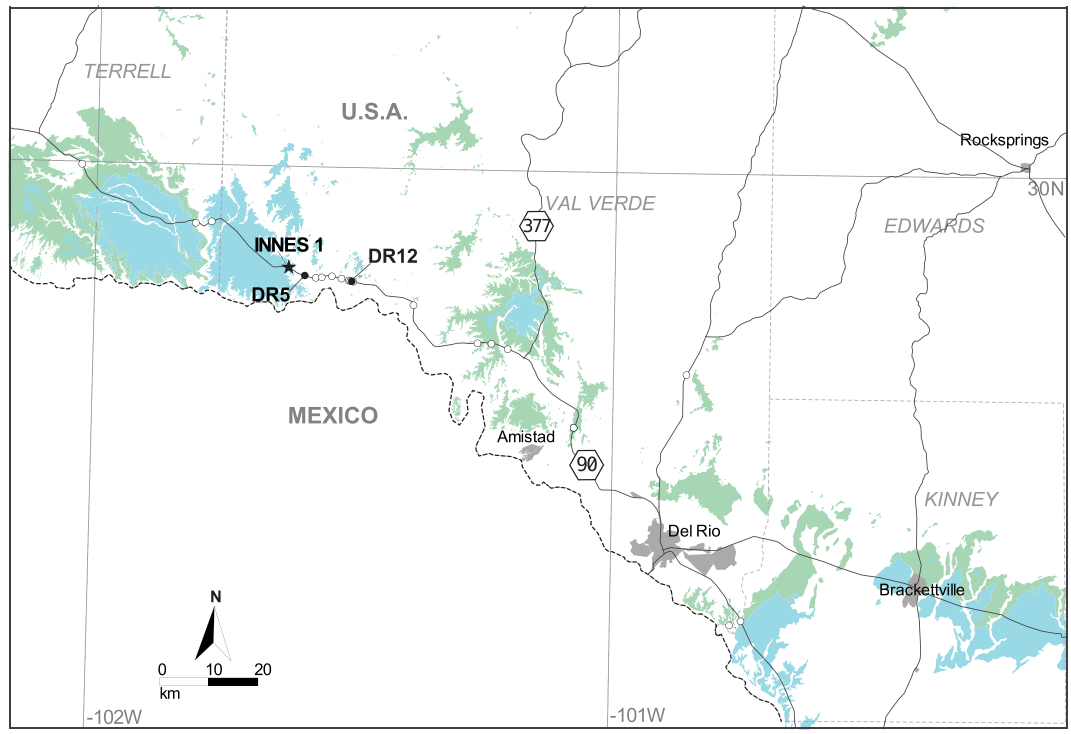

Figure 1. Location of the studied Innes-1 core (star, 29.831244 lat., −101.626078 long.) and outcrops DR5 (filled circle, 29.816835 lat., −101.596273 long.) and DR12 (filled circle, 29.809300 lat., −101.508867 long.). Open circles represent the locations of the outcrops studied by Minisini et al. (2018). Figure modified from Eldrett et al. (2017). Blue shading indicates outcrops of the Austin Chalk and green shading indicates outcrops of the Eagle Ford.

3. Results and Discussion

3.1. Loss of Isotopically Heavy Rhenium During Oxidative Weathering

Unweathered core samples from Innes-1 have an average OC concentration of ∼3% (Figures 2 and 3). Variably weathered samples from outcrop sections DR5 and DR12 correlate to overlapping parts of the Lower Eagle Ford succession sampled by Innes-1 and have average OC concentrations of 0.3% and 0.1%, respectively, meaning that >90% of the organic C has been lost. We infer that Re has been lost alongside the oxidation of OC to CO_2, as suggested by direct field measurements of mudrock weathering (Roylands et al., 2022). The average Re concentration of the Innes-1 samples is 80 ng g^{-1}, albeit with significant stratigraphic variability (±58 ng g^{-1}, 1 S.D.) (Figures 2 and 3). Outcrop samples from DR5 and DR12 have Re concentrations of ∼11 and 14 ng g^{-1}, respectively, meaning that >90% of Re has been lost. Repeating the Re loss calculation using Re/Ti ratios to account for rock mass loss during oxidation produces an estimate of ∼83% total Re loss, which is similar. The high degree of Re loss observed in the Eagle Ford samples is similar to previous studies of Re mobility in weathered sedimentary successions, with estimates of 25%–64%, 99% and 93% in the Ohio Shale, Utica Shale and New Albany Shale, respectively (Jaffe et al., 2002; Miller et al., 2015; Peucker-Ehrenbrink & Hannigan, 2000). The ratio of Re loss to OC loss is ∼2.4×10^{-6} g g^{-1}.

We observed different mean δ^{187}Re compositions for unweathered and weathered samples (Figure 3). The average δ^{187}Re of samples from the Innes-1 drillcore is −0.52 ± 0.16‰ (1 S.D., n = 16), while the average δ^{187}Re of samples from DR5 and DR12 are −0.73 ± 0.15‰ (1 S.D., n = 8) and −0.86 ± 0.36‰ (1 S.D., n = 16) respectively. Remarkably, the 0.3 ‰ shift to lower δ^{187}Re in the weathered samples is statistically identical to the shift observed by Miller et al. (2015) in the New Albany Shale, where unweathered samples had an average δ^{187}Re composition of −0.55 ± 0.05‰ and weathered samples were −0.75 ± 0.14‰. The data are also consistent with Dellinger et al. (2021), who found a correlation between the fractional loss of Re and δ^{187}Re compositions of "gray" shale river sediments from the Mackenzie River catchment, that was taken to indicate a loss of isotopically heavy Re during oxidative weathering of these rocks. The robust primary observation from this study alongside

10.1029/2024GC011795

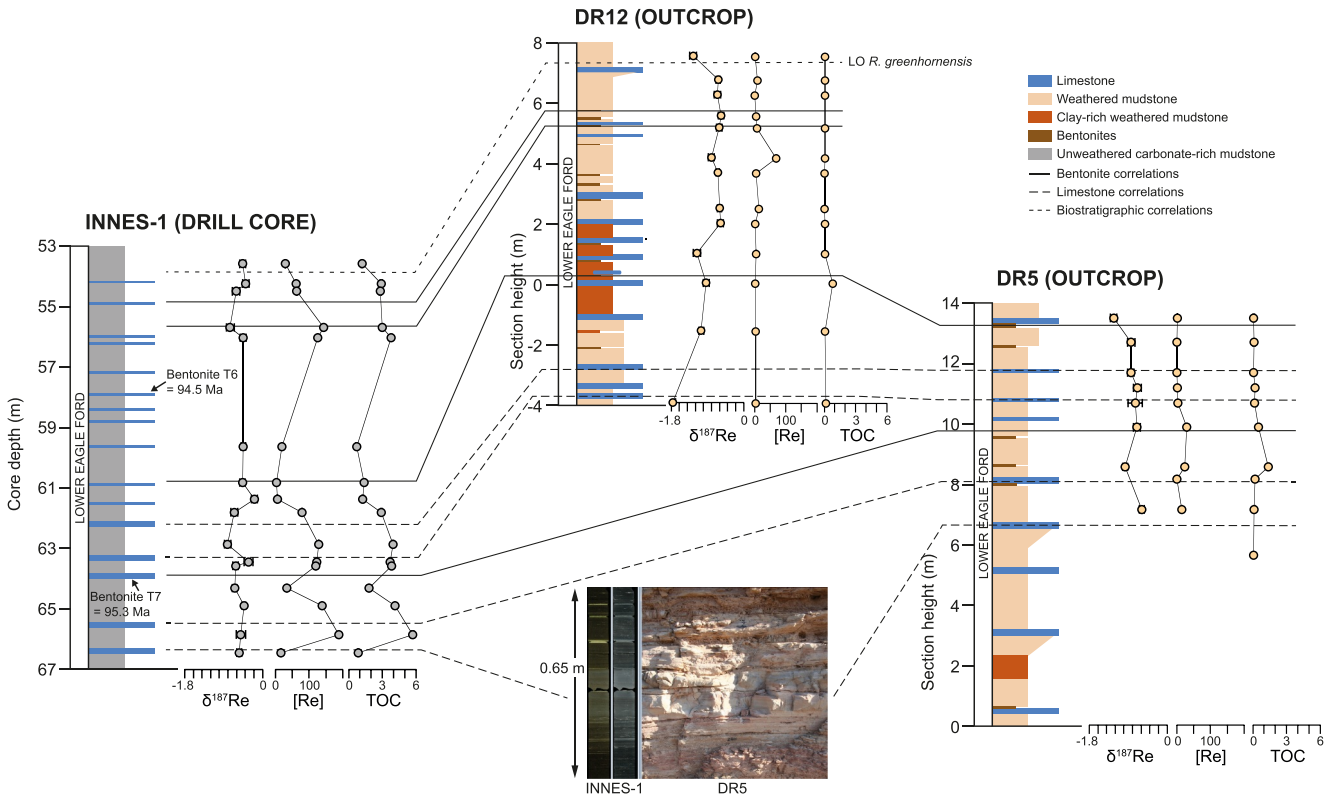

Figure 2. Correlation of the stratigraphic successions recorded in the Innes-1 core and outcrops DR5 and DR12. Correlation lines are taken from Minisini et al. (2018) and are based on limestone (long dashes) and bentonites (solid lines). The ages of key bentonite beds are shown for reference. Rhenium concentrations are in units of ng g^{-1} and TOC is wt%. The photo shows the similarity between beds exposed at outcrop DR5 (6–7 m height) and in core Innes-1 (66.75–66.10 m depth). Yellow-fluorescing facies are bentonite beds that provide clear marker horizons across southern Texas and guide the correlation of laterally extensive limestone beds (Minisini et al., 2018).

Table 1
Correlation of Samples From the Innes-1 Core and Outcrops DR5 and DR12

Innes-1 sample depth (m)	DR5 sample height (m)	DR12 sample height (m)
53.65		7.6
54.30		6.8
54.55		6.3, 5.6
55.74		5.2
56.08		5.2, 5.6
59.66		1.0, 2.0, 2.5, 3.7
60.85	13.4	0.0
61.39	12.6	0.0
61.83	11.6	0.0, −1.6
62.88	11.1	
63.46	10.6, 9.8	
63.59	10.6, 9.8	
64.32	9.8, 8.5	
64.90	8.5	
65.85	7.1	
66.45	7.1, 8.1	

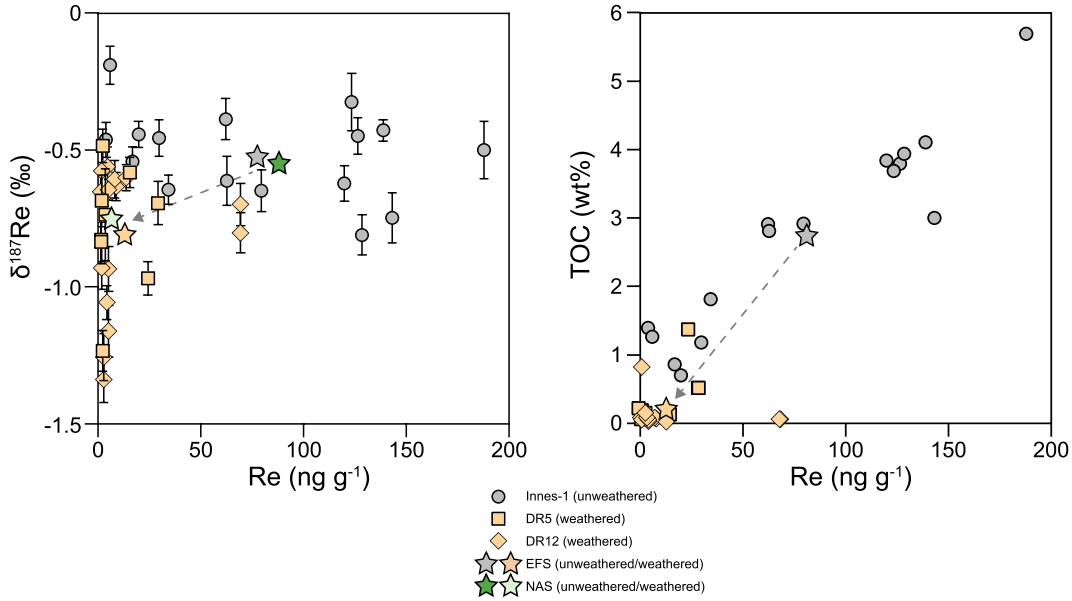

Figure 3. Relationships between Re concentrations, Re isotope compositions and OC content of sedimentary rock samples obtained from the Innes-1 core and outcrops DR5 and DR12. Innes-1 data (gray circles) and outcrop data (orange squares and diamonds). Stars indicate the means of the weathered and unweathered sample sets. The average weathered and unweathered compositions of the New Albany Shale (NAS, Miller et al., 2015) are shown for comparison in the left panel. EFS: Eagle Ford Shale. Green shading shows the location of Eagle Ford surface outcrops, and blue shading indicates outcrops of the overlying Austin Chalk.

previous efforts, therefore, is that oxidative weathering leads to a preferential loss of isotopically heavy Re in the mobile, soluble phase, leaving the near-completely oxidized residue isotopically light by a few tenths of per mil.

3.2. δ^{187}Re Composition of Weathered Rhenium Correlates to Weathering Intensity

While the formation-scale observations allow us to conclude on the direction of isotopic fractionation during weathering, they do not allow us to investigate whether there are systematic changes in the composition of weathered Re with the degree of Re removal (weathering intensity). The lithostratigraphic framework of the Eagle Ford Group allows us to determine which outcrop samples are coeval with specific unweathered core samples, and thus to calculate the fractional loss of Re:

$$\text{Fraction of Re loss} = \frac{(\text{Re}_{\text{rock}} - \text{Re}_{\text{residue}})}{\text{Re}_{\text{rock}}} \quad (1)$$

and the δ^{187}Re composition of this flux:

$$\delta^{187}\text{Re}_{\text{weathered}} = \frac{\left(\delta^{187}\text{Re}_{\text{rock}} * \text{Re}_{\text{rock}}\right) - \left({}^{187}\text{Re}_{\text{residue}} * \text{Re}_{\text{residue}}\right)}{\text{Re}_{\text{weathered}}} \quad (2)$$

where $\text{Re}_{\text{weathered}}$ is the weathered flux of Re transported away from the starting rock (Re_{rock}), leaving a pool of unmobilized Re in the rock residue ($\text{Re}_{\text{residue}}$). Sample pairs were identified by matching unweathered samples from the Innes-1 core to the nearest 1, 2, or 3 samples (depending on the precision of the correlation framework) in the correlative interval of outcrops DR5 and DR12 (Figure 2, Table 1). Since the Eagle Ford Group is characterized by significant lithostratigraphic and chemostratigraphic variability over length scales of cm to m (Eldrett et al., 2015; Minisini et al., 2018), this exercise carries inherent uncertainty that affects the detail of the $\delta^{187}\text{Re}_{\text{weathered}}$ calculations. However, changing the sample pairs by matching to alternative nearest neighbors does not alter the sense of the results. Additionally, similar trends are obtained by calculating $\delta^{187}\text{Re}_{\text{weathered}}$ from formation-scale averages of the data set (Figure 4), and thus the sense of the results are robust even if the fine details may be subject to small changes.

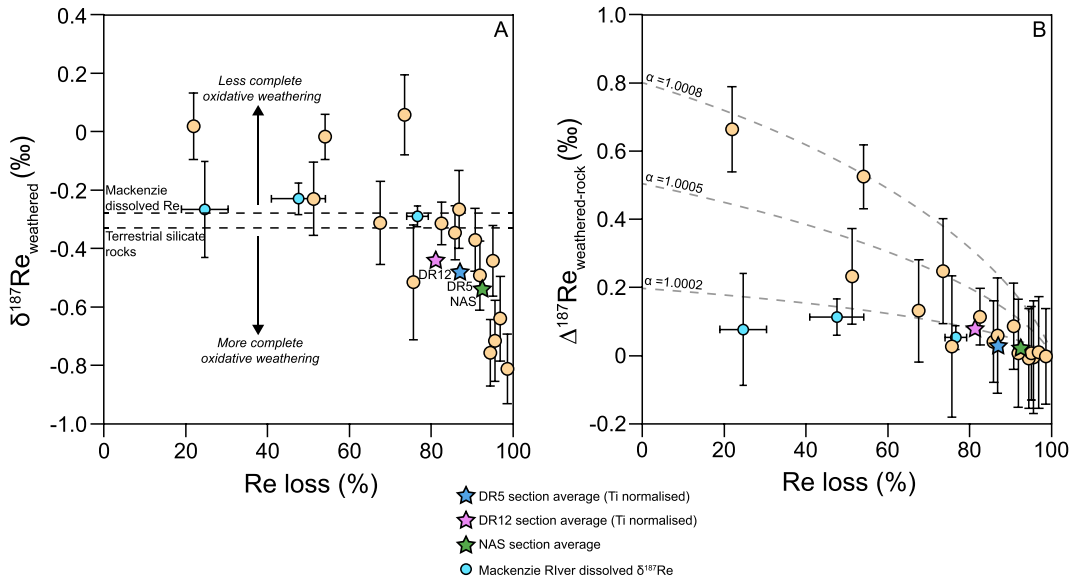

Figure 4. Relationship of $\delta^{187}Re_{weathered}$ and oxidative weathering intensity (Re loss) in Eagle Ford sedimentary rocks. (a) Isotope composition of weathered Re ($\delta^{187}Re_{weathered}$) calculated using Equation 2. (b) Isotope composition of weathered Re normalized to the unweathered starting composition ($\Delta^{187}Re_{weathered\text{-}rock}$). Stars are the section averages for the fractional loss of Re, $\delta^{187}Re_{weathered}$ and $\Delta^{187}Re_{weathered\text{-}rock}$ from this study and from Miller et al. (2015) (NAS: New Albany Shale). Rayleigh fractionation lines are calculated assuming open-system behavior using $\alpha = R_1/R_2$, where R_1 is the $^{187}Re/^{185}Re$ ratio of "weathered" Re and R_2 is the $^{187}Re/^{185}Re$ ratio of the unweathered rock. Blue circles are the calculated $\delta^{187}Re_{weathered}$ and $\Delta^{187}Re_{weathered\text{-}rock}$ values for dissolved Re in the Mackenzie River catchment (Dellinger et al., 2021).

The results of the calculations are plotted in Figure 4a, and show a trend from higher $\delta^{187}Re_{weathered}$ compositions at lower fractional loss of Re to lower compositions with more complete loss of Re. Since the data set is drawn from a stratigraphic succession spanning approximately one million years (Eldrett et al., 2015), $\delta^{187}Re_{weathered}$ in Figure 4a is also affected by long-term variability in the $\delta^{187}Re$ of the unweathered Innes-1 deposits. To correct for this variability, $\delta^{187}Re_{weathered}$ compositions are corrected to the $\delta^{187}Re$ of the unweathered sample:

$$\Delta^{187}Re_{weathered-rock} = \delta^{187}Re_{weathered} - \delta^{187}Re_{rock} \quad (3)$$

where $\Delta^{187}Re_{weathered\text{-}rock}$ is the corrected weathering flux. These calculations are shown in Figure 4b. They are notable for $\Delta^{187}Re_{weathered\text{-}rock}$ being>0.6‰ higher than the unweathered rock at Re loss <40% and approaching 0‰ at Re loss >90%; that is, the weathered flux has the same composition as the unweathered rock, $\delta^{187}Re_{weathered\text{-}rock} = \delta^{187}Re_{rock}$. This observation hints at an open-system Rayleigh-type behavior, where the progressive loss of Re to oxidative weathering slowly brings the accumulated weathered flux toward the starting composition of the unweathered substrate. This behavior can be empirically described by alpha fractionation factors between 1.0002 and 1.0008 (Figure 4b). While useful for quantitative modeling of Re weathering processes, these values carry no assumption of what process(es) may be driving this behavior or indeed what Re phase(s) may be mobilized during oxidation.

The various possibilities for what process(es) may be driving Re isotope variability during oxidative weathering have been discussed previously by Miller et al. (2015) and Dellinger et al. (2021) and the main options are briefly summarized here. Firstly, Re may be fractionated during oxidation, a process which ab initio calculations of equilibrium Re isotope compositions at different oxidation states (IV and VII) suggest is possible. Specifically, Re(VII) species tend to have higher predicted $\delta^{187}Re$ compositions than reduced Re(IV) species (Miller et al., 2015). While it has been proposed that much of the sedimentary inventory of Re may be sourced from thiolated species derived from ReO_4^-(VII) (Helz & Dolor, 2013; Miller et al., 2015), reduction may nonetheless occur post-burial in a manner similar to that proposed for molybdenum (Dahl et al., 2013). Secondly, Re may be liberated from different sedimentary fractions, with the most labile fractions having the highest $\delta^{187}Re$ compositions and the more recalcitrant fractions retaining lower compositions. We cannot resolve which of these

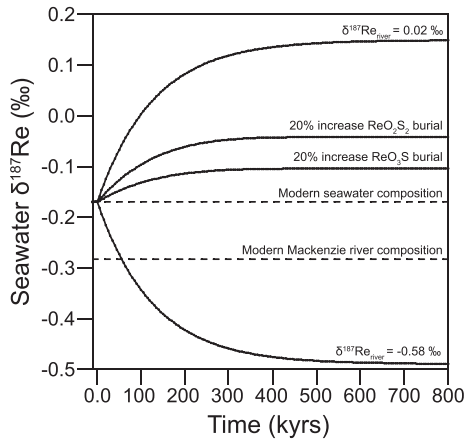

Figure 5. Box model showing the evolution of seawater δ^{187}Re in response to changes in the composition of Re weathering from continental rocks and due to changes in the burial flux of thiolated Re into seafloor sediments. The modern seawater composition is −0.17‰ (Dickson et al., 2020) and the Mackenzie River composition is −0.28‰ (Dellinger et al., 2021), close to the Re isotope composition of crustal silicate rocks (~−0.33‰, Wang et al., 2023).

mechanisms explains the observed Re isotope trends at present, although we note that organic-rich rocks contain a highly heterogenous mix of sedimentary fractions that might lean in favor of the second option, a conclusion also reached by Dellinger et al. (2021). We note that the trend of dissolved Re versus calculated Re loss from the Mackenzie River catchment plots follows a slightly different trend from the Eagle Ford data, albeit consistent with the lower fractionation factor of 1.0002 (Dellinger et al., 2021; Figure 4b). This difference hints at the possibility that the different mechanisms governing Re release may have varying levels of importance in different areas, presumably due to variations in Re host phases, lithology, climatology, erosion rates etc. It should be noted, however, that the Mackenzie values are calculated relative to a homogenous basin starting endmember which may mask some of the natural variation in weathering processes. Regardless, determining the exact mechanism(s) behind Re fractionation during rock weathering remains a topic for future investigation.

An intriguing observation from the data we present is that calculated $\delta^{187}Re_{weathered}$ for near-complete Re oxidation from organic-rich rocks is much lower than the composition of dissolved Re in the only river system yet measured (Dellinger et al., 2021, see Figure 4a). This difference shows that oxidative weathering may not be currently limited by erosion rate (i.e., supply of unaltered material), as commonly assumed in some models of Phanerozoic climate change (e.g., Berner, 2006; Bolton et al., 2006; we note that some incorporate a feedback mechanism to vary organic carbon weathering (e.g., Lenton et al., 2018)). However, this observation comes with the caveat that the bedrock Re-isotope compositions of the Eagle Ford and Mackenzie catchments may be dissimilar (e.g., weathering may be rate-limited in the Mackenzie catchment but not in the Eagle Ford) or that higher than global average rates of erosion in the Mackenzie catchment (Carson et al., 1998) are responsible for the relatively elevated δ^{187}Re compositions seen there. Nonetheless, if our results prove to be more widely applicable, they would imply that modern oxidative weathering is broadly sensitive to weathering kinetics, as demonstrated experimentally by Soulet et al. (2021), who showed a relationship between CO_2 emissions from oxidative rock weathering and temperature.

3.3. Weathering Intensity as a Lever to Alter Oceanic δ^{187}Re

We use a simple box model to explore the effect of changing the isotope composition of the input flux of Re (due to weathering intensity) to the oceans on seawater δ^{187}Re (Figure 5). In this model, the 4.3×10^5 mol yr^{-1} flux of Re to the modern ocean mainly from rivers (Miller et al., 2011) is given a δ^{187}Re composition of −0.28‰, the mean value of dissolved Re in the Mackenzie River (Dellinger et al., 2021), the only such study published to date. This input flux is balanced by an equivalent removal into seafloor sediments, which is divided into two types: an oxic flux, whose magnitude is equivalent to ~30,000 mol yr^{-1} estimated by Sheen et al. (2018); and a "low-oxygen" flux as either ReO_3S or ReO_2S_2. The size of the thiolated removal term is scaled to completely balance the input flux. Thiolated Re species were chosen as no direct Re isotope measurements of modern marine sediments exist, yet these species have published ab initio calculations of their isotopic composition (ReO_3S: −0.33‰; ReO_2S_2: −0.64‰, Miller et al., 2015) and may contribute a large proportion of Re burial in low-oxygen sediments (e.g., Helz & Dolor, 2013). The model is equilibrated with a modern seawater Re inventory of 5.477×10^{10} mol with a δ^{187}Re of −0.17‰ (Dickson et al., 2020).

Instantaneously changing the riverine input by ±0.3‰ (i.e., the approximate range observed in Figure 4b) induces a change in seawater δ^{187}Re of several tenths of per mil, which gradually equilibrates over ~400 Kyrs. The range of variation is larger than the typical uncertainty on δ^{187}Re ± 0.05–0.1‰ (Dellinger et al., 2020; Miller et al., 2009) and thus measurable, subject to an appropriate sedimentary or mineral archive of ancient seawater Re being identified. Changing the size of the "low oxygen" Re removal flux by 20%, a magnitude typical of other redox-sensitive elements during Phanerozoic deoxygenation events (Clarkson et al., 2018; Dickson, 2017) also induces changes in seawater δ^{187}Re, though of a lower magnitude to the variation induced by weathering (Figure 5). The model indicates that the Re isotope proxy should be able to resolve variations in ancient weathering intensity even during periods of major environmental upheaval when Re burial fluxes may have become altered.

4. Conclusions

Our study of Late-Cretaceous organic rich rocks in the Eagle Ford Group allows us to draw three primary conclusions: (a) Oxidative weathering of organic-rich sedimentary rocks mobilizes isotopically heavy Re that drives the oxidized rock residue to lighter compositions. (b) Re mobilized from sedimentary rocks at low weathering intensity appears to be systematically heavier than Re mobilized at higher weathering intensity. This trend may be explained by either equilibrium fractionation during oxidative weathering and/or incongruent dissolution. (c) The variation observed in the composition of weathered Re is large enough to alter the global seawater Re isotope composition over geological timescales that is large enough to be detected by current analytical approaches. Our study contributes to an emerging picture of the Re isotope system as a potential tool to reconstruct oxidative weathering intensity, and hence CO_2 emissions, during ancient climate events, given a suitable archive of ancient seawater Re isotope compositions can be identified.

Data Availability Statement

Data are openly available as an online supplement to this paper and via the Natural Environment Research Council National Geoscience Data Centre (Dickson et al., 2024).

Acknowledgments
This study was funded by the Natural Environment Research Council Grant NE/T001119. James Brakeley is acknowledged for laboratory technical support and Erdem Idiz is acknowledged for assistance curating the samples used in this study. We thank Shell Plc. for providing the sample material.

References

Archer, D. (2005). Fate of fossil fuel CO_2 in geologic time. *Journal of Geophysical Research*, *110*(C9), C09S05. https://doi.org/10.1029/2004JC002625

Berner, R. A. (2006). GEOCARBSURF: A combined for Phanerozoic atmospheric O_2 and CO_2. *Geochimica et Cosmochimica Acta*, *70*(23), 5653–5664. https://doi.org/10.1016/j.gca.2005.11.032

Birck, J.-L., Roy Barman, M., & Capmas, F. (1997). Re-Os isotopic measurements at the femtomole level in natural samples. *Geostandards Newsletter*, *21*(1), 19–27. https://doi.org/10.1111/j.1751-908x.1997.tb00528.x

Bolton, E. W., Berner, R. A., & Petsch, S. T. (2006). The weathering of sedimentary organic matter as a control on atmospheric CO_2: II. Theroetical modelling. *American Journal of Science*, *306*(8), 575–615. https://doi.org/10.2475/08.2006.01

Carson, M. A., Jasper, J. N., & Conly, F. M. (1998). Magnitude and sources of sediment input to the Mackenzie Delta, Northwest Territories, 1974–94. *Arctic*, *51*(2), 116–124. https://doi.org/10.14430/arctic1053

Clarkson, M. O., Stirling, C. H., Jenkyns, H. C., Dickson, A. J., Porcelli, D., Moy, C. M., et al. (2018). Uranium isotope evidence for two episodes of deoxygenation during Oceanic Anoxic Event 2. *Proceedings of the National Academy of Sciences of the United States of America*, *115*(12), 2918–2923. https://doi.org/10.1073/pnas.1715278115

Dahl, T. W., Chappaz, A., Fitts, J. P., & Lyons, T. W. (2013). Molybdenum reduction in a sulfidic lake: Evidence from X-ray absorption fine-structure spectroscopy and implications for the Mo paleoproxy. *Geochimica et Cosmochimica Acta*, *103*, 213–231. https://doi.org/10.1016/j.gca.2012.10.058

Dalai, T. K., Singh, S. K., Trivedi, J. R., & Krishnaswami, S. (2002). Dissolved rhenium in the Yamuna river system and the Ganga in the Himalaya: Role of black shale weathering on the budgets of Re, Os and U in rivers and CO_2 in the atmosphere. *Geochimica et Cosmochimica Acta*, *66*(1), 29–43. https://doi.org/10.1016/s0016-7037(01)00747-5

Dellinger, M., Hilton, R. G., Baronas, J. J., West, A. J., Burt, E. I., Clark, K. E., et al. (2023). High rates of rock organic carbon oxidation sustained as Andean sediment transits the Amazon foreland-floodplain. *Proceedings of the National Academy of Sciences of the United States of Ameica*, *120*(39), e2306343120. https://doi.org/10.1073/pnas.2306343120

Dellinger, M., Hilton, R. G., & Nowell, G. M. (2020). Measurements of rhenium isotopic composition in low-abundance samples. *Journal of Analytical Atomic Spectrometry*, *35*(2), 377–387. https://doi.org/10.1039/c9ja00288j

Dellinger, M., Hilton, R. G., & Nowell, G. M. (2021). Fractionation of rhenium isotopes in the Mackenzie River basin during oxidative weathering. *Earth and Planetary Science Letters*, *573*, 117131. https://doi.org/10.1016/j.epsl.2021.117131

Dickson, A., Hilton, R., Prytulak, J., Minisini, D., Eldrett, J., Dellinger, M., et al. (2024). Rhenium isotope compositions of the Eagle Ford Shale [Dataset]. *NERC EDS National Geoscience Data Centre*. https://doi.org/10.5285/e047ed34-1d9d-4079-be72-1e9027cbb380

Dickson, A. J. (2017). A molybdenum isotope perspective on Phanerozoic deoxygenation events. *Nature Geoscience*, *10*, 721–726. https://doi.org/10.1038/ngeo3028

Dickson, A. J., Hsieh, Y.-T., & Bryan, A. L. (2020). The rhenium isotope composition of Atlantic Ocean seawater. *Geochimica et Cosmochimica Acta*, *287*, 221–228. https://doi.org/10.1016/j.gca.2020.02.020

Eldrett, J. S., Dodsworth, P., Bergman, S. C., Wright, M., & Minisini, D. (2017). Water-mass evolution in the Cretaceous Western Interior Seaway of North America and equatorial Atlantic. *Climate of the Past*, *13*(7), 855–878. https://doi.org/10.5194/cp-13-855-2017

Eldrett, J. S., Ma, C., Bergman, S. C., Lutz, B., Gregory, F. J., Dodsworth, P., et al. (2015). An astronomically calibrated stratigraphy of the Cenomanian, Turonian and earliest Coniacian from the Cretaceous Western Interior Seaway, USA: Implications for global chronostratigraphy. *Cretaeceous Research*, *56*, 316–344. https://doi.org/10.1016/j.cretres.2015.04.010

Helz, G., & Dolor, M. K. (2013). What regulates rhenium deposition in euxinia basins? *Chemical Geology*, *204–305*, 131–141.

Hilton, R. G., Gaillardet, J., Calmels, D., & Birck, J.-L. (2014). Geological respiration of a mountain belt revealed by the trace element rhenium. *Earth and Planetary Science Letters*, *403*, 27–36. https://doi.org/10.1016/j.epsl.2014.06.021

Hilton, R. G., Turowski, J. M., Winnick, M., Dellinger, M., Schleppi, P., Williams, K. H., et al. (2021). Concentration-discharge relationships of dissolved rhenium in alpine catchments reveal its use as a tracer of oxidative weathering. *Water Resources Research*, *57*(11), e2021WR029844. https://doi.org/10.1029/2021WR029844

Hilton, R. G., & West, A. J. (2020). Mountains, erosion and the carbon cycle. *Nature Reviews Earth & Environment*, *1*(6), 284–299. https://doi.org/10.1038/s43017-020-0058-6

Hollingsworth, E. H., Elling, F. J., Badger, M. P. S., Pancost, R. D., Dickson, A. J., Rees-Owen, R. L., et al. (2024). Spatial and temporal patterns in petrogenic organic carbon mobilisation during the Paleocene-Eocene Thermal Maximum. *Paleoceanography and Paleoclimatology*, *39*(2), e2023PA004773. https://doi.org/10.1029/2023PA004773

Horan, K., Hilton, R. G., Dellinger, M., Tipper, E., Galy, V., Calmels, D., et al. (2019). Carbon dioxide emissions by rock organic carbon oxidation and the net geochemical carbon budget of the Mackenzie River basin. *American Journal of Science*, *319*(6), 473–499. https://doi.org/10.2475/06.2019.02

Jaffe, L. A., Peucker-Ehrenbrink, B., & Petsch, S. T. (2002). Mobility of rhenium, platinum group elements and organic carbon during black shale weathering. *Earth and Planetary Science Letters*, *198*(3–4), 339–353. https://doi.org/10.1016/s0012-821x(02)00526-5

Lenton, T. M., Daines, S. J., & Mills, B. J. W. (2018). COPSE reloaded: An improved model of biogeochemical cycling over Phanerozoic time. *Earth-Science Reviews*, *178*, 1–28. https://doi.org/10.1016/j.earscirev.2017.12.004

Lyons, S. L., Baczynski, A. A., Babila, T. L., Bralower, T. J., Hajek, E. A., Kump, L. R., et al. (2017). Paleocene-Eocene Thermal Maximum prolonged by fossil carbon oxidation. *Nature Geoscience*, *12*(1), 54–60. https://doi.org/10.1038/s41561-018-0277-3

Miller, C. A., Peucker-Ehrenbrink, B., & Ball, L. (2009). Precise determination of rhenium isotope composition by multi-collector inductively-coupled plasma mass spectrometry. *Journal of Analytical Atomic Spectrometry*, *24*(8), 1069–1078. https://doi.org/10.1039/b818631f

Miller, C. A., Peucker-Ehrenbrink, B., & Schauble, E. A. (2015). Theoretical modeling of rhenium isotope fractionation, natural variations across a black shale weathering profile, and potential as a paleoredox proxy. *Earth and Planetary Science Letters*, *430*, 339–348. https://doi.org/10.1016/j.epsl.2015.08.008

Miller, C. A., Peucker-Ehrenbrink, B., Walker, B. D., & Marcantonio, F. (2011). Re-assessing the surface cycling of molybdenum and rhenium. *Geochimica et Cosmochimica Acta*, *75*(22), 7146–7179. https://doi.org/10.1016/j.gca.2011.09.005

Minisini, D., Eldrett, J. S., Bergman, S. C., & Forkner, R. (2018). Chronostratigraphic framework and depositional environments in the organic-rich, mudstone-dominated Eagle Ford Group, Texas, USA. *Sedimentology*, *65*(5), 1520–1557. https://doi.org/10.1111/sed.12437

Peucker-Ehrenbrink, B., & Hannigan, R. E. (2000). Effects of black shale weathering on the mobility of rhenium and platinum group elements. *Geology*, *28*(5), 475–478. https://doi.org/10.1130/0091-7613(2000)28<475:eobswo>2.0.co;2

Roylands, T., Hilton, R. G., Garnett, M. H., Soulet, G., Newton, J.-A., Peterkin, J. L., & Hancock, P. (2022). Capturing the short-term variability of carbon dioxide emissions from sedimentary rock weathering in a remote mountainous catchment, New Zealand. *Chemical Geology*, *608*, 121024. https://doi.org/10.1016/j.chemgeo.2022.121024

Sheen, A. L., Kendall, B., Reinhard, C. T., Creaser, R. A., Lyons, T. W., Bekker, A., et al. (2018). A model for the oceanic mass balance of rhenium and implications for the extent of Proterozoic ocean anoxia. *Geochimica et Cosmochimica Acta*, *227*, 75–95. https://doi.org/10.1016/j.gca.2018.01.036

Soulet, G., Hilton, R. G., Garnett, M. H., Roylands, T., Klotz, S., Croissant, T., et al. (2021). Temperature control on CO_2 emissions from the weathering of sedimentary rocks. *Nature Geoscience*, *14*(9), 665–671. https://doi.org/10.1038/s41561-021-00805-1

Walker, J. C. G., Hays, P. B., & Kasting, J. F. (1981). A negative feedback mechanism for the long-term stabilization of Earth's surface temperature. *Journal of Geophysical Research*, *86*(C10), 9776–9782. https://doi.org/10.1029/jc086ic10p09776

Wang, W., Dickson, A. J., Stow, M. A., Dellinger, M., Burton, K. W., Savage, P. S., et al. (2023). Rhenium elemental and isotopic variations at magmatic temperatures. *Geochemical Perspective Letters*, *28*, 48–53. https://doi.org/10.7185/geochemlet.2402

Zondervan, J. R., Hilton, R. G., Dellinger, M., Clubb, F. J., Roylands, T., & Ogrič, M. (2023). Rock organic carbon oxidation CO_2 release offsets silicate weathering sink. *Nature*, *623*(7986), 329–333. https://doi.org/10.1038/s41586-023-06581-9